

A theoretical and experimental analysis of frequency transfer uncertainty, including frequency transfer into TAI*

Gianna Panfilo¹ and Thomas E Parker²

¹ International Bureau for Weights and Measures (BIPM), Sèvres, France

² National Institute of Standards and Technology (NIST), Boulder, CO, USA


Received 22 January 2010, in final form 21 July 2010

Published 8 September 2010

Online at stacks.iop.org/Met/47/552

Abstract

Results are presented from a theoretical and experimental investigation of the frequency transfer uncertainty (FTU) in long-distance comparisons of frequency standards. The FTU can be an important component of the total uncertainty in such comparisons. The use of the Allan deviation in characterizing the FTU is analysed theoretically and it is shown that for certain noise types the Allan deviation is biased high. A potentially more accurate first difference statistic that can be used in certain situations is also discussed. In addition, an experimental determination of the noise types and levels in common transfer techniques is presented. It is shown that FTUs approaching 1 part in 10^{16} at 30 days are possible with current transfer methods. Finally, a method is presented for estimating the FTU in calibrating International Atomic Time (TAI) with a primary frequency standard.

 Online supplementary data available from stacks.iop.org/Met/47/552/mmedia

(Some figures in this article are in colour only in the electronic version)

1. Introduction

Recent reductions in the frequency uncertainty of primary frequency standards through the use of caesium fountains have resulted in the uncertainty introduced by the frequency transfer process becoming a significant component of the total uncertainty of long-distance comparisons. This also includes the calibration of International Atomic Time (TAI) [1–3] with a primary standard. Remote standards are commonly compared using time links such as GPS common view (GPS CV), GPS carrier phase (GPS CP) and two-way satellite time and frequency transfer (TWSTFT). Surprisingly, there has not yet been a thorough investigation of how to characterize the frequency uncertainty introduced by the transfer process. Magnitudes and types of noise processes involved need to be determined as well as the best way to quantify the introduced frequency uncertainty. With the development of new ultra-stable optical frequency standards the transfer process is becoming even more important.

Two basic approaches are used to determine the noise introduced by a long-distance time or frequency transfer

process. In situations where quiet clocks, such as hydrogen masers, are used the transfer noise is quite often larger than the clock noise at time intervals less than ~ 5 days. Also the transfer noise processes are usually of a different type than the clock noise. In such cases the transfer noise can be determined independently of the clock noise at short time intervals. In general, the transfer noise at time intervals longer than ~ 5 days can only be determined if there are two or more independent transfer processes available. In this case the clock noise can be eliminated by performing a double difference (clock A minus clock B compared by method 1 minus method 2) resulting in a time series made up of just the transfer noises from the two transfer methods. Once the transfer noise processes have been isolated, appropriate statistical techniques can be employed to characterize the frequency uncertainty that is introduced.

This paper presents the results of both theoretical and experimental investigations of frequency transfer uncertainty (FTU). In section 2 a theoretical analysis is carried out to determine the analytical expressions for the FTU, expressed in terms of the Allan deviation, for white phase noise (WPN), flicker phase noise (FPN) and white frequency (random walk phase) noise, which are noise types commonly

* US government work, not subject to US copyright.

involved in frequency transfer [4]. For WPN and white frequency noise (WFN) the analysis is based on the law of propagation of uncertainties [5] applied to an average frequency calculated for a specific time interval, and use of the appropriate autocorrelation functions [6, 7]. In the case of FPN the autocorrelation functions are determined by spectral analysis [8]. It is shown that the Allan deviation is biased high for WPN and FPN, but corrections can be made. The Allan deviation is unbiased only for WFN. The approach using the Allan deviation is necessary when only one transfer process is available and consequently the transfer noise must be quantified in the presence of clock frequency offsets and clock noise. Though the standard deviation is used in section 2 as a theoretical tool to obtain the true FTU, it is not appropriate to use the standard deviation in real world situations where only one transfer process is available. Here clock noise processes such as flicker frequency and random walk frequency will make the value of the standard deviation dependent on the length of the data set. The Allan deviation, with proper corrections, must be used.

In section 3 a first difference statistic introduced in [1] that can be used when two independent transfer processes are available is reviewed and expanded upon. In this situation the standard deviation (calculated as a function of averaging time τ) could be used, but as discussed in section 3 the first difference statistic, $\sigma_{ft}(A, \tau)$, is a better tool.

In section 4 typical noise types and noise levels in real long-distance time (frequency) transfer links are examined in detail. Section 5 considers the FTU for calibrations of TAI.

2. Theory

2.1. Definitions

The instantaneous output voltage of a precision oscillator [9, 10] can be expressed as

$$V(t) = (V_0 + \varepsilon(t)) \sin(2\pi \nu_0 t + \phi(t)),$$

where V_0 is the nominal peak voltage amplitude, $\varepsilon(t)$ is the deviation from the nominal amplitude, ν_0 is the nominal frequency and $\phi(t)$ is the phase deviation from the nominal phase $2\pi \nu_0 t$. The frequency instability of a precision oscillator is defined in terms of the instantaneous, normalized frequency deviation, $y(t)$, as follows:

$$y(t) = \frac{\nu(t) - \nu_0}{\nu_0} = \frac{\dot{\phi}(t)}{2\pi \nu_0},$$

where $\nu(t)$ is the instantaneous frequency (time derivative of the phase divided by 2π) and

$$\dot{\phi}(t) = \frac{d\phi(t)}{dt}.$$

The phase instability, defined in terms of the phase deviation $\phi(t)$, can also be expressed in units of time, as

$$x(t) = \frac{\phi(t)}{2\pi \nu_0}.$$

With these definitions, the instantaneous, fractional frequency deviation is

$$y(t) = \frac{dx(t)}{dt}.$$

In particular we define the mean fractional frequency deviation over the time interval τ as

$$\bar{y}(t) = \frac{x(t) - x(t - \tau)}{\tau}. \quad (1)$$

2.2. FTU in terms of the Allan deviation

Two different methods are used to obtain the uncertainty of (1) in terms of the Allan deviation. The first is based on the law of propagation of uncertainty using appropriate models of stochastic processes and the second is based on spectral analysis. We prefer to use a mathematical model when it is available, but for FPN there is no simple mathematical model available. For this case, a semi-empirical model has been used.

2.2.1. Law of propagation of uncertainty. Considering the relation between phase and frequency expressed in (1), it is possible to apply the law of propagation of uncertainty [5] to $\bar{y}(t)$, and we obtain

$$u_{\bar{y}(t)}^2 = \frac{u_{x(t)}^2 + u_{x(t-\tau)}^2 - 2u_{(x(t),x(t-\tau))}}{\tau^2}, \quad (2)$$

where $u_{\bar{y}(t)}^2$ is the variance (squared uncertainty) of $\bar{y}(t)$. $u_{\bar{y}(t)}$ is the FTU if the noise process under consideration originates in the frequency transfer procedure being used. To calculate (2) we have to know the variance, $u_{x(t)}^2$, and covariance, $u_{(x(t),x(t-\tau))}$, in terms of the phase (time) measurements.

The covariance term [6] for a random process $X(t)$ is defined as

$$u_{(X(t_1),X(t_2))} = \text{Cov}(X(t_1), X(t_2)) = E([X(t_1) - E(X(t_1))][X(t_2) - E(X(t_2))]) \quad (3)$$

but in the literature [7] it often refers to the autocorrelation function given by

$$R_X(t_1, t_2) = E(X(t_1)X(t_2)), \quad (4)$$

where t_1 and t_2 are arbitrary sampling times and the functional $E(\cdot)$ is the expectation value.

Functions (3) and (4) are identical for zero mean frequency processes, which is the case for all the noise processes considered in this investigation. The autocorrelation function indicates to what extent the process is correlated with itself at two different times. If the process is stationary the autocorrelation functions (4) depend only on the time difference $\tau = t_2 - t_1$. Thus, R_X reduces to a function of just the time difference variable τ , that is,

$$R_X(\tau) = E(X(t)X(t - \tau)), \quad (5)$$

where t_1 is now denoted as just t and t_2 is $(t - \tau)$. Stationarity assures us that the expectation value is not dependent on t . For almost all stationary data, the average values computed over an

ensemble at time t_1 will equal the corresponding average values computed over a time history record (the ergodic theorem).

However, the autocorrelation function R_X can also be obtained by the inverse Fourier transform of the spectral density $S_y(f)$ [11, 12],

$$R_X(\tau) = \int_0^\infty \left(\frac{S_y(f)}{(2\pi f)^2} \right) \cos(2\pi f \tau) df. \quad (6)$$

In many situations the stochastic processes are not stationary and the integral from zero to infinity in (6) is not convergent. To avoid this problem we considered the limited frequency range [12] $f_l < f < f_h$ where f_l is the lowest frequency and may be taken to be much smaller than the reciprocal of the longest time of interest and f_h is the high-frequency necessary for convergence of the integral. We call $2\pi f_l = \varepsilon$ and $2\pi f_h = \omega$. In practice, the random fluctuations can often be represented by the sum of five noise processes assumed to be independent [9, 13], as

$$S_y(f) = \sum_{\alpha=-2}^2 h_\alpha f^\alpha \quad 0 < f < f_h, \quad (7)$$

where h_α is a constant and α is an integer. Corresponding to different values of α we have different noises: for $\alpha = -2$ we have random walk frequency noise (RWFN); for $\alpha = -1$ flicker frequency noise (FFN); for $\alpha = 0$ WFN; for $\alpha = 1$ FPN and for $\alpha = 2$ WPN. From relations (6) and (7) we obtain

$$R_X(\tau) = \sum_{\alpha=-2}^2 \int_{\varepsilon\tau}^{\omega\tau} \frac{h_\alpha u^{\alpha-2}}{(2\pi)^{\alpha+1}} \tau^{1-\alpha} \cos(u) du = \sum_{\alpha=-2}^2 R_\alpha(\tau), \quad (8)$$

where $u = 2\pi f \tau$ and the expression is different for each noise denoted with $\alpha = -2, -1, 0, 1, 2$.

However, relation (8) is very divergent, so we introduce a less divergent function called $I(\tau)$ [8]:

$$I(\tau) = \sum_{\alpha=-2}^2 \int_{\varepsilon\tau}^{\omega\tau} \frac{h_\alpha u^{\alpha-2}}{(2\pi)^{\alpha+1}} \tau^{1-\alpha} (1 - \cos(u)) du = \sum_{\alpha=-2}^2 I_\alpha(\tau). \quad (9)$$

This function takes on different expressions for each different noise type (different values of α).

To obtain the variance and covariance terms in (2) we must know the stochastic processes used to model the noise types [14, 15]. This is easily done for WPN and WFN. To obtain the frequency uncertainty for FPN we will use the method in section 2.2.2.

2.2.2. *Spectral analysis.* The uncertainty of (1) can be expressed using the link between autocorrelation functions and spectral density functions using the inverse Fourier transform [11, 12]. The uncertainty is obtained using equation (5) and incorporating the decomposition presented in (8) and (9):

$$\begin{aligned} u_{\bar{y}(t)}^2 &= E \left(\left(\frac{x(t) - x(t - \tau)}{\tau} \right)^2 \right) = \frac{2}{\tau^2} [R_X(0) - R_X(\tau)] \\ &= \frac{2}{\tau^2} [R_\alpha(0) - R_\alpha(\tau)] = \frac{2I_\alpha(\tau)}{\tau^2}, \end{aligned} \quad (10)$$

where $I_\alpha(\tau) = R_\alpha(0) - R_\alpha(\tau)$. In this expression we use the function $I_\alpha(\tau)$ because it is a less divergent function than $R_\alpha(\tau)$ as explained in [8]; here some divergent terms in $R_\alpha(\tau)$ are reduced because of the difference with $R_\alpha(0)$. Also the expression for the Allan variance can be obtained using the function $I_\alpha(\tau)$:

$$\sigma_y^2(\tau_0) = \frac{4I_\alpha(\tau_0) - I_\alpha(2\tau_0)}{\tau_0^2}. \quad (11)$$

Dividing (10) with (11) we obtain a relation for the squared frequency uncertainty in terms of the Allan variance:

$$u_{\bar{y}(t)}^2 = \frac{2I_\alpha(\tau)/\tau^2}{(4I_\alpha(\tau_0) - I_\alpha(2\tau_0))/\tau_0^2} \sigma_y^2(\tau_0), \quad (12)$$

τ_0 is the time interval where the Allan variance is known (from, for example, an experimental measurement). Equation (12) provides the relation between the FTU and Allan variance for every value of τ , using the theoretical outcome reported in (10).

Using relation (12) we can evaluate the FTU for all different noise types (it is possible to find related expressions of $I_\alpha(\tau)$ in [8]) but as explained above we use relation (12) to obtain the FTU for FPN. The FTU for the WFN and the WPN will be analysed using the stochastic process approach.

2.3. FTU in terms of the Allan deviation

Following the methods presented in the previous sections we obtain expressions for the frequency uncertainty in a time transfer link in terms of the Allan deviation for WPN, WFN and FPN. Note below that only for WFN is the FTU equal to the Allan deviation, $\sigma_y(\tau)$. For WPN and FPN the FTU is smaller than $\sigma_y(\tau)$.

2.3.1. *White phase noise.* WPN can be modelled as random independent numbers fitting a Gaussian distribution, $X(t) \sim N(0, \sigma^2)$, where σ^2 is the variance and the mean is equal to zero. The covariance in the case of WPN is equal to zero and the relationship between the Allan variance, calculated for the relative frequency differences, $\sigma_y^2(\tau_0)$ and σ^2 is given by the relation $\sigma^2 = \sigma_y^2(\tau_0)\tau_0^2/3$. This relation can be obtained using the definition of the Allan variance and by following the method shown in [16, 17].

Applying (2), the frequency uncertainty is given by

$$u_{\bar{y}(t)}^2 = \frac{\sigma^2 + \sigma^2}{\tau^2} = 2 \frac{\sigma^2}{\tau^2} = \frac{2}{3} \frac{\sigma_y^2(\tau_0)\tau_0^2}{\tau^2}. \quad (13)$$

where τ_0 is the time interval between measurements and $\tau = \tau_0, 2\tau_0, 3\tau_0, \dots$ as typically used in the Allan variance. In (13) we use τ_0 and τ to distinguish the behaviour of the Allan variance from the behaviour of the FTU. Considering that the Allan variance cannot distinguish the clock contribution from the time transfer contribution for $\tau > 10$ days, the FTU can be obtained from (13) with only one value of the Allan variance at τ_0 .

Assuming $\tau_0 = \tau$ and assuming the knowledge of the Allan variance for a long period we obtain

$$u_{\bar{y}(\tau)}^2 = \frac{2}{3} \sigma_y^2(\tau), \quad (14)$$

where $u_{y(\tau)}$ is the FTU. Thus we see that for WPN the Allan deviation alone would give a value for the FTU that is about 22% too high. Note that (14) gives the FTU only in the region of τ where transfer noise dominates.

2.3.2. *White frequency (random walk phase) noise.* To model WFN we use a Brownian motion (or Wiener process) approach [6, 14, 18]. The Wiener process indicated by $W(t)$ is defined as a Gaussian Markov process with independent increments whose basic parameters are the drift μ and the diffusion coefficient σ [6, 14, 18]. Considering the definition of the Wiener process, given by the solution of the stochastic differential equation

$$dX_t = \mu dt + \sigma dW(t), \tag{15}$$

the solution, considering $W(0) = 0$, of (15) [12] can be written as

$$X_t = \mu t + \sigma W(t). \tag{16}$$

At any instant the standard Wiener process is described by a Gaussian distribution

$$X_t \sim N(\mu t, \sigma^2 t).$$

where σ has the dimension $T^{1/2}$. In particular we have that the variance of this process is $\text{Var}(X_t) = \sigma^2 t$ and the covariance is $\text{Cov}(X_t, X_s) = \sigma^2 \min(t, s)$. The diffusion coefficient σ^2 is linked to the Allan variance [16, 17] by the relation $\sigma^2 = \sigma_y^2(\tau_0)\tau_0$. Therefore, using the values for the variance and the covariance of WFN, the frequency uncertainty in the case of $\mu = 0$ and applying (2) is

$$u_{\bar{y}(t)}^2 = \frac{\sigma^2 t + (t - \tau)\sigma^2 - 2(t - \tau)\sigma^2}{\tau^2} = \frac{\sigma^2}{\tau} = \frac{\sigma_y^2(\tau_0)\tau_0}{\tau}. \tag{17}$$

In this case for $\tau_0 = \tau$ we have

$$u_{\bar{y}(\tau)}^2 = \sigma_y^2(\tau). \tag{18}$$

Thus we see that for white frequency (random walk phase) transfer noise the Allan deviation is the FTU. Again (18) gives the FTU only for the region of τ dominated by transfer noise.

2.3.3. *Flicker phase noise.* To obtain the FTU for FPN we use relation (12). For FPN the function $I_\alpha(\tau)$ is given in [8] as

$$I_1(\tau) = \frac{h_1}{2\pi} \int_{\varepsilon\tau}^{\omega_n\tau} \frac{1 - \cos(u)}{u} du \tag{19}$$

$$= \frac{h_1}{(2\pi)^2} (\gamma + \ln(\omega_n\tau) - \text{Ci}(\omega_n\tau)),$$

where the dependence on ω_n is given by the divergence at infinity of the cosine integral function [19], for which a standard expansion is $\text{Ci}(x) = \gamma + \ln(x) - \int_0^x (1 - \cos(u))/u du$, and γ is Euler's constant equal to 0.577 21. This expression is not divergent at zero so we can

consider the integral limit 0 instead of $\varepsilon\tau$. In this case the squared frequency uncertainty is

$$u_{\bar{y}(t)}^2 = \frac{2(\gamma + \ln(\omega_n\tau) - \text{Ci}(\omega_n\tau))}{3\gamma + 3 \ln(\omega_n\tau_0) - \ln(2) - 4\text{Ci}(\omega_n\tau_0) + \text{Ci}(2\omega_n\tau_0)} \times \frac{\tau_0^2}{\tau^2} \sigma_y^2(\tau_0). \tag{20}$$

In the case of $\tau_0 = \tau$ the result is

$$u_{\bar{y}(t)}^2 = \frac{2(\gamma + \ln(\omega_n\tau) - \text{Ci}(\omega_n\tau))}{3\gamma + 3 \ln(\omega_n\tau) - \ln(2) - 4\text{Ci}(\omega_n\tau) + \text{Ci}(2\omega_n\tau)} \times \sigma_y^2(\tau). \tag{21}$$

In this case the frequency uncertainty depends on ω_n , which is related to the measurement bandwidth. In general the product $\omega_n\tau$ is not considered in the analytical relations of [20] because, if $\omega_n\tau \gg 1$, a more simplified relation can be obtained. In our case relation (20) would be approximated by the relation

$$u_{\bar{y}(\tau)}^2 = \frac{2}{3} \frac{\sigma_y^2(\tau_0)\tau_0^2}{\tau^2},$$

which is equal to (13) obtained for WPN. In relations (20) and (21) for FPN we cannot assume $\omega_n\tau \gg 1$ and (13) would not be correct. To obtain a value for ω_n different methods must be used. Using the analytical expression for the Allan variance in the case of FPN [8, 10] an approximate result is obtained. Using the Nyquist frequency and the sampling theorem an analytical expression, confirmed from the approximated one, is obtained where $\omega_n = \pi/\tau_0$. In the case of real flicker phase transfer noise processes where $\tau_0 = 1$ day the value for $\omega_n\tau_0$ is equal to π . In this case the term presented in (21)

$$\frac{2(\gamma + \ln(\omega_n\tau_0) - \text{Ci}(\omega_n\tau_0))}{3\gamma + 3 \ln(\omega_n\tau_0) - \ln(2) - 4\text{Ci}(\omega_n\tau_0) + \text{Ci}(2\omega_n\tau_0)}$$

has a value of 0.79. Thus for FPN, for this case, we obtain

$$u_{\bar{y}(\tau)}^2 \cong 0.79\sigma_y^2(\tau). \tag{22}$$

Again (22) gives the FTU only for the region of τ dominated by transfer noise.

2.3.4. *Examples of calculations of the FTU from simulated and real data.* Examples of calculations comparing the true frequency uncertainty from the standard deviation to that obtained with (14), (18) and (22) are shown in the supplementary data available at stacks.iop.org/Met/47/552/mmedia.

3. FTU from a first difference statistic

In 1998 a first difference statistic was briefly introduced to quantify the FTU in a time series [1]. Here we will consider it in more detail. For noise types where the mean frequency is zero (white phase, flicker phase and white frequency), this first difference statistic is statistically equivalent to the fractional frequency uncertainties calculated by the standard deviations in section 2. When two independent transfer techniques are available between the same two frequency sources one can take the difference of the two time series (one from each transfer technique) and obtain a new time series that removes the clock

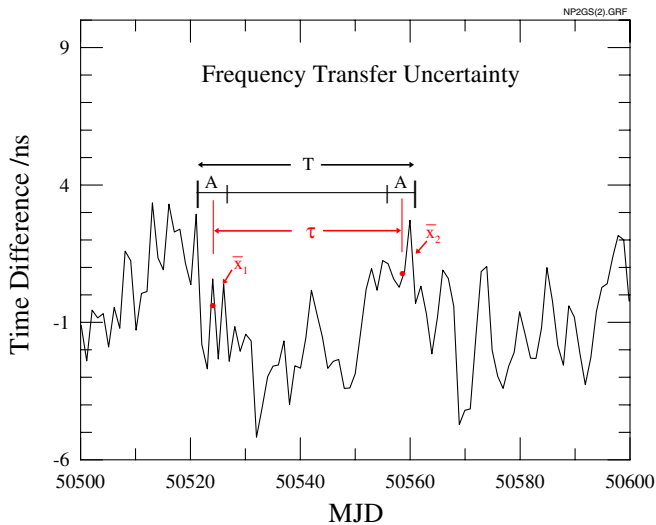


Figure 1. Illustration of how $\sigma_{ft}(A, \tau)$, FTU, is calculated from a double difference data set. \bar{x} is the average phase over the interval A .

noises and frequency offset and just contains the combined noise of the two transfer techniques. We refer to this as a double difference. The first difference statistic of [1] can be used to calculate the FTU from double differenced time series data and is a very useful tool in helping to determine the noise level and noise type of frequency transfer instabilities at long time intervals. This first difference statistic, called $\sigma_{ft}(A, \tau)$ here, is defined by the following relation, and its calculation is illustrated in figure 1:

$$\sigma_{ft}^2(A, \tau) = \frac{\langle (\bar{x}_{i+\tau} - \bar{x}_i)^2 \rangle}{\tau^2} = \frac{1}{\tau^2 n} \sum_{i=1}^n (\bar{x}_{i+\tau} - \bar{x}_i)^2, \quad (23)$$

where \bar{x}_i is the average of a double difference of phase (time difference) values obtained with two different transfer techniques over interval A at epoch i and τ is the interval between epoch i and $i + \tau$. $\sigma_{ft}(A, \tau)$ is just the root mean square (RMS) frequency of the time series at interval τ . $\sigma_{ft}(A, \tau)$ can be used in a meaningful way only in situations where there is no clock frequency offset or clock noise. As was shown in section 2, an uncorrected Allan deviation calculation on the same time series is biased approximately 12% to 22% high for FPN and WPN, respectively.

$\sigma_{ft}(A, \tau)$ is the true frequency transfer error even in the presence of a non-zero mean. Any value of $(x_{i+\tau} - x_i)/\tau = y_i$ that is not zero constitutes a real frequency error introduced by the transfer systems. In the absence of known biases (a bias would be a non-zero average slope in the time series or equivalently a non-zero mean frequency), the frequency transfer error obtained with $\sigma_{ft}(A, \tau)$ is the FTU. The standard deviation (calculated as a function of τ) would not see this bias. In principle, a known bias could be measured and corrected for, in which case the FTU would be the RMS deviation about the bias (this would be equivalent to the standard deviation in section 2). An example of a bias might be part of an annual cycle in transfer delay that could have a nearly linear component over an interval of several months. Another example might be an ageing mechanism in one of

the components of a transfer system that could look like a linear (or nearly linear) change in delay over a period of time. If biases are present that are poorly understood (and hence uncorrectable) then the frequency transfer error of $\sigma_{ft}(A, \tau)$ should be considered the FTU.

The Allan deviation could be used on a double difference data set, but there are several advantages to using $\sigma_{ft}(A, \tau)$ rather than the Allan deviation to calculate the FTU. First of all $\sigma_{ft}(A, \tau)$ is unbiased for transfer noises, whereas the Allan deviation alone is approximately 12% to 22% too large for FPN and WPN, and is correct only for WFN, as shown in section 2. This difference can be understood because the Allan deviation is a good estimator for frequency instability in time transfer or clock data, but it is not always a good estimator for the frequency uncertainty. Also, the confidence limits are better for $\sigma_{ft}(A, \tau)$ than for the Allan deviation. Expressions for the confidence limits of $\sigma_{ft}(A, \tau)$ are presented in the supplementary data. In addition, $\sigma_{ft}(A, \tau)$, being a first difference statistic, will be sensitive to slow time delay changes in the transfer systems that look like a frequency offset and are real errors. The Allan deviation, being a second difference, will not see these errors. The Allan deviation by itself is a convenient tool to use, but bias corrections must be made for accurate results. The main disadvantage with $\sigma_{ft}(A, \tau)$ is that it cannot be used in situations where only one time transfer technique is available. Here, the time series between two clocks contains clock frequency offset and clock noise. In such cases (14), (18) and (22), which use the Allan deviation, should be used.

A comparison has been made between $\sigma_{ft}(A, \tau)$ and the FTU calculated from (14) and (22) using simulated data in a manner similar to section 1A in the supplementary data. Simulated time series of WPN and FPN data containing 1×10^5 data points were generated and analysed. For WPN the results for $\sigma_{ft}(A, \tau)$ and the FTU calculated from (14) are essentially identical, with differences less than 0.1% at all values of τ from τ_0 to $25\,000\tau_0$. A similar procedure was carried out for FPN and the results agreed to within a few per cent.

4. Experimental observations of the FTU for different transfer techniques

In sections 4 and 5 we will examine different techniques for determining the type and magnitude of the noise processes that cause FTU in several real time links. Figure 2 shows the time deviation, TDEV, of UTC(NIST) – UTC(USNO) for two different links over a two year period in 2005 and 2006. NIST is the National Institute of Standards and Technology in Boulder, CO, USA, and USNO is the US Naval Observatory in Washington, DC, USA. One link is a direct, relatively short baseline, GPS CV link, shown as (blue) diamonds, using multi-channel receivers and the International GNSS Service (IGS) ionosphere models. The other is an indirect TWSTFT link via PTB (Physikalisch-Technische Bundesanstalt in Braunschweig, Germany), shown as (red) circles. The two-way links from the NIST to PTB and PTB to USNO were both at Ku-band using the communications satellite Intelsat 707. There is currently no direct two-way

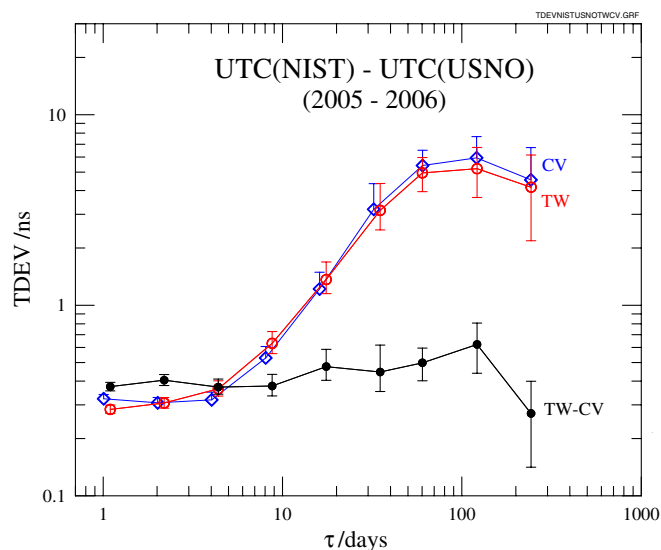


Figure 2. Time deviation plots of UTC(NIST) – UTC(USNO) as observed with GPS CV (blue) diamonds and TWSTFT via PTB (red) circles. The solid dots are for the double difference TWSTFT minus common view.

link between NIST and USNO. All data are for 1 day averages. Since the clocks are maser ensembles at both ends (and hence very quiet) the TDEVs at τ less than about 3 days are dominated by transfer noise, and hence both the GPS CV and TWSTFT links show transfer noise, which is flicker phase in nature at a level of about 300 ps. It is certain that this is transfer noise since it is much too large and of the wrong noise type to be clock noise (the clock noise is flicker frequency for τ in the range of 1 to 3 days). At τ values larger than about 3 days the TDEV shows clock noise. The GPS CV and TWSTFT curves are not identical because both time series have some missing data that is not the same for the two links. The decrease in the TDEV for the GPS CV and TWSTFT data for τ larger than 100 days occurs because both UTC(NIST) and UTC(USNO) are steered to UTC, Coordinated Universal Time. These data represent an example where the transfer noise can be observed at short time intervals when quiet clocks are being used.

When the time series for TWSTFT and GPS CV are differenced (now a double difference) the long-term clock noise is removed and TDEV, shown as (black) dots in figure 2, is much lower at τ greater than 5 days. The TWSTFT–GPS CV TDEV curve represents the combined transfer noise of TWSTFT and GPS CV (assuming TWSTFT and GPS CV are independent and largely uncorrelated) and it is roughly flicker in nature at a level of about 400 ps essentially for all τ values. The small bump near 150 days in the TWSTFT–GPS CV curve is probably an indication of an annual cycle in the time delay of one or both transfer systems.

Data such as the double difference in figure 2 can be used to calculate the FTU. Figure 3 shows the combined FTU of TWSTFT and GPS CV as calculated from $\sigma_{ft}(A = 1 \text{ d}, \tau)$ for NIST–PTB links using the double difference of TWSTFT minus GPS CV, over the two year interval (730 days) covering the years 2005 and 2006 (upper (blue) curve with solid dots). From TDEV data (not shown) it is clear that the FTU in figure 3 for NIST–PTB is dominated at small τ by the noise in common

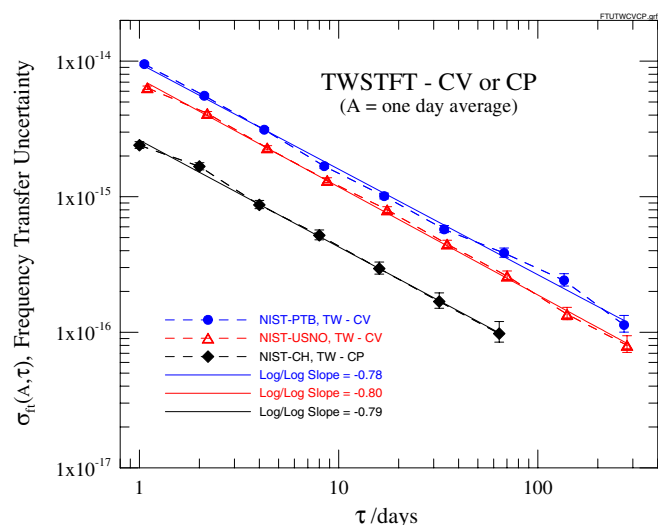


Figure 3. Examples of $\sigma_{ft}(A, \tau)$, FTU, as a function of τ for several different frequency transfer methods over links for NIST–PTB, NIST–USNO and NIST–CH. Data are shown for double differences. The transfer methods are GPS CV (CV above), GPS CP (CP above) and TWSTFT (TW above). Linear log/log slopes are indicated by the solid lines. All data are for a two year interval in 2005 and 2006, except for the NIST–CH data which are for a 184 day interval in 2006.

view. The value of TDEV at 1 day for TWSTFT between NIST and PTB is about 150 ps (with masers at both ends) while for common view the TDEV at 1 day is about 500 ps. The NIST–USNO plot (middle (red) curve with hollow triangles) is for TWSTFT minus GPS CV and comes from the same time series data as used for figure 2. Again this is for the two year period of 2005 and 2006. $\sigma_{ft}(A = 1 \text{ d}, \tau)$ is about 30% lower here than for the NIST–PTB link. The noise for NIST–USNO is lower primarily because of the better (shorter) GPS CV link. The NIST–CH plot (lower (black) curve with solid diamonds) is for TWSTFT minus GPS CP between NIST and the Swiss Federal Office of Metrology, METAS, and is from data supplied by Christine Hackman [21]. The NIST–CH data are for an interval of only 184 days in 2006. This link exhibits the lowest noise mainly because carrier phase is more stable than code-based common view. Note that the slopes for the three curves are all nearly the same, reflecting the fact that all the link instabilities are close to flicker phase in nature, as indicated by the double difference curve in figure 2. Though it is not obvious from the curves in figure 3, a $\sigma_{ft}(A, \tau)$ curve for FPN noise is not a straight line on a log/log plot. See section 4A in the supplementary data for more details.

The TWSTFT links NIST–PTB and NIST–CH are very similar, and therefore the lower (black) curve in figure 3 indicates that the upper (blue) curve is dominated by GPS CV at all values of τ . Therefore, one can conclude that the FTU for transatlantic GPS CV is about 1×10^{-14} at 1 day and 7×10^{-16} at 30 days. The τ dependence is about $\tau^{-0.78}$, indicating that the instabilities are FPN in nature. The FTU for the combined TWSTFT and GPS CV transfer techniques in the NIST–USNO link is about 30% smaller and has a similar dependence on τ . However, because the GPS CV and TWSTFT have similar levels, it is difficult to draw any definite conclusions about the

individual techniques. The combined noise of TWSTFT and GPS CP gives the lowest FTU of about 2.5×10^{-15} at 1 day and just less than 2×10^{-16} at 30 days. The τ dependence is about $\tau^{-0.79}$, which is similar to that of the other two curves. Some other TWSTFT and GPS CP links have shown a somewhat less steep τ dependence [21]. TDEV values at 1 day (not shown) for the GPS CP and TWSTFT data in the lower curve are nearly the same (with GPS CP being slightly smaller), again making it difficult to draw any definite conclusions about the individual techniques. However, as shown in [3] it is not necessary to fully characterize the individual techniques in order to make definitive statements about a comparison uncertainty. If the noise processes in the two transfer techniques are independent (uncorrelated), the uncertainty of an unweighted average of the frequency differences obtained from each transfer technique individually will be one half of the calculated $\sigma_{ft}(A, \tau)$ at the appropriate τ interval. Under the best of circumstances, using currently available frequency transfer techniques, it would take well over 300 days to reach FTUs approaching 1×10^{-17} .

5. Estimating FTU when only one transfer path is available

If only one transfer path is available the task of determining the FTU at long time intervals becomes more difficult. An example of this is reporting the results of a Cs fountain primary frequency standard into TAI. TAI is a ‘paper’ time scale and does not physically exist in a single location. Although many different transfer techniques are used to transfer clock data through a complex network for use in TAI, there is, in effect, only one transfer path linking any particular laboratory to TAI. In this type of situation the transfer noise level and noise type must be estimated because they are largely obscured by clock noise. In some cases the clock noise is sufficiently small at short time intervals that TDEV can be used to directly observe the transfer noise at small τ values, as in figure 2. However, this does not give much information about the noise level and noise type at longer averaging times. Closure measurements provide some information, but they do not identify the noise characteristics between a specific pair of stations, and they may not include certain site-dependent instabilities [22].

5.1. Frequency transfer into TAI

In 2005 the Bureau International des Poids et Mesures, BIPM, began publishing in *Circular T* [23] the type A uncertainties, $u_A(k)_i$, of UTC – UTC(k) for each laboratory k reporting clock data into TAI [22]. This prompted the Consultative Committee for Time and Frequency (CCTF) Working Group on Primary Frequency Standards to re-examine the expression used to calculate the FTU of a primary frequency standard reporting into TAI. Another motivating factor was evidence that time transfer instabilities had been decreasing with the use of improved time transfer techniques. Figure 4 shows TDEV plots from a comparison between the post-processed maser ensemble AT1E at NIST and TAI for two different periods. The upper (blue) curve with dots covers a 1.5 year period from November 1999 to May 2001. The TDEV values

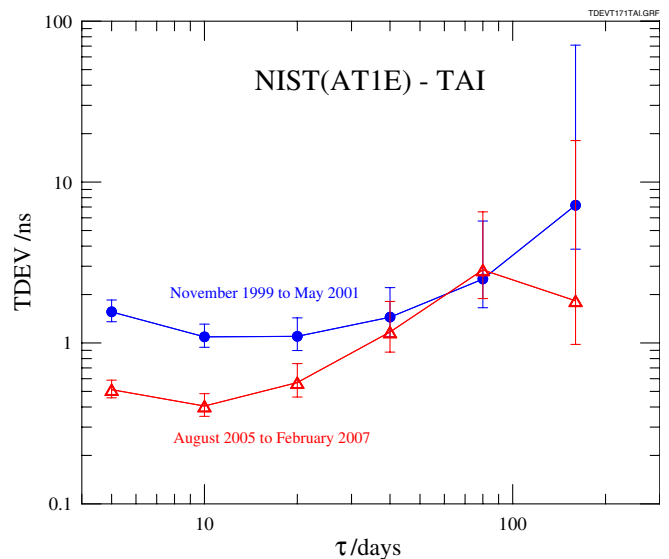


Figure 4. Time deviation for a comparison between the maser ensemble, AT1E, at NIST and TAI over an 18 month period around the year 2000, (blue) dots, and a similar period around the year 2006, (red) triangles. The decrease in TDEV at small values of τ is due to improved time/frequency transfer.

for τ in the range of 5 to 20 days represent transfer noise because they are too high to be clock noise, and the noise type is not WFN or FFN, as would be expected for clock noise. The lower (red) curve with triangles also shows TDEV for a 1.5 year interval around 2006. Over the 6 year period from 2000 to 2006 the transfer noise at $\tau = 5$ days has been reduced by about a factor of 3 through the increased use of multi-channel GPS CV receivers, IGS measured ionosphere delay corrections, P3 (a two-frequency, P code technique) and improved TWSTFT. (As of 2010 there has been no additional decrease.) The TDEV values at $\tau = 5$ and 10 days for the lower curve still represent time transfer noise. Though clock noise makes it difficult to identify the transfer noise type, the fact that TDEV decreases between $\tau = 5$ and $\tau = 10$ days indicates that there is some WPN present. In contrast, the data of figures 2 and 3 would suggest that instabilities in the most common transfer techniques are mostly FPN, even beyond 100 days. Transfer noise into TAI is obviously a unique situation because of the complex way TAI is calculated, and the large number of stations and great variety of equipment involved [22]. Therefore, it is not surprising that the noise characteristics might be different. This clearly is an area that needs further investigation.

Figure 5 shows Allan deviation plots from the same time series data that were used for figure 4. The improvement by a factor of 3 at small τ values is also clear here. The straight (black) line illustrates the old formula (see (24) in the following subsection) used to calculate the FTU, $u_{1/TAI}$, for primary frequency standards. The Allan deviation and expressions (14), (18) and (22) of section 2 must be used here to estimate FTU because these are data between two clocks. For τ in the range of 5 to 10 days the transfer noise appears to be a combination of WPN and FPN. Thus the Allan deviation in figure 5 must be decreased by about 17% to obtain the FTU.

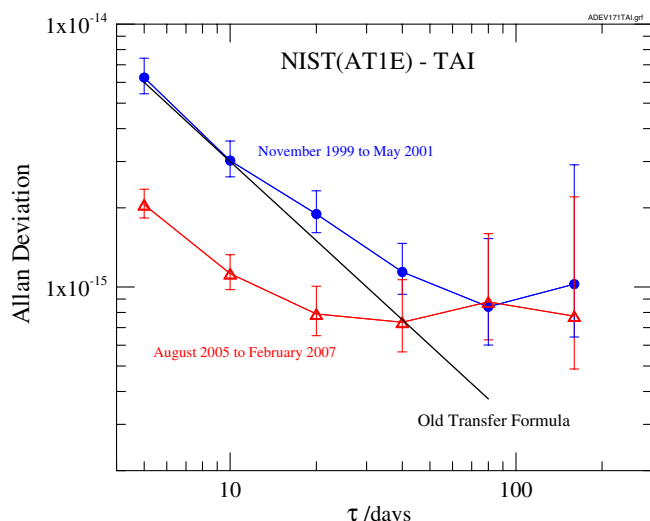


Figure 5. Allan deviation for a comparison between the maser ensemble, AT1E, at NIST and TAI over an 18 month period around the year 2000, (blue) dots, and a similar period around the year 2006, (red) triangles. The decrease in Allan deviation at small values of τ is due to improved time/frequency transfer. The straight (black) line with no data points represents the FTU from the old formula used by the BIPM.

As can be seen in figure 5, the old formula, based on single-channel GPS CV time transfer, was a reasonably good estimate of FTU around the year 2000. However, by 2006 it was clear that a new expression for FTU was needed. Furthermore, the values of $u_A(k)$ now published in *Circular T* are available. These values are estimated for each laboratory and eliminate a problem with the old formula in that the same expression was used for all laboratories reporting primary standards. Differing $u_A(k)$ values in *Circular T* make it clear that the transfer uncertainty is not always the same for each laboratory (a number of different transfer techniques are in use).

5.2. New frequency transfer equation

Equation (24) is the expression used by the BIPM until September 2006 to calculate the fractional FTU, $u_{I/TAI}$, introduced by the time transfer process when reporting a primary frequency standard measurement to TAI (black straight line in figure 5).

$$u_{I/TAI} = \frac{3 \times 10^{-14}}{\tau/\text{day}} \quad (\text{In other words } u_{I/TAI} = \text{FTU}). \quad (24)$$

The same expression was used for all labs and the $1/\tau$ dependence is that expected for WPN. In September 2006 a new expression was adopted at the recommendation of the CCTF Working Group on Primary Frequency Standards. This expression is

$$u_{I/TAI} = \left(\frac{\sqrt{u_A(k)_1^2 + u_A(k)_2^2}}{\tau_0} \right) / \left(\frac{\tau}{\tau_0} \right)^x. \quad (25)$$

Here $u_A(k)_i$ is the type A uncertainty (in seconds) of UTC – UTC(k) for station k at epoch i as reported in *Circular T*. $\tau_0 = 4.32 \times 10^5$ s (5 days) and is the data interval of UTC – UTC(k)

in *Circular T*. $\tau = t_2 - t_1$ and is the report interval for the primary frequency standard. The value of the exponent x is currently 0.9. A value of x less than 1 was chosen to more accurately reflect the fact that there is a significant component of FPN in the time transfer instabilities. In this situation the FTU beyond about 10 days can only be estimated based on data such as those shown in figures 2 and 3.

Equation (25) as currently used to estimate the FTU for primary frequency standards should be considered a work in progress and may very well have to be modified in the future. These modifications may involve the introduction of a bias term and changes in the value of x as more is learned about the instabilities in time/frequency transfer techniques.

6. Conclusions

Theoretical techniques for characterizing FTU have been developed in terms of the Allan deviation for situations where clock frequency offsets and noise are present. Here, the transfer noise can be isolated at short time intervals if quiet clocks are available. The Allan deviation at short time intervals is an accurate measure of the FTU only for white frequency (random walk phase) noise. For WPN and FPN the Allan deviation is biased high, but correction factors have been calculated. A first difference statistic has also been discussed which should be used when no clock offset and noise are present, as when a double difference can be performed. Much has been learned in this investigation about the noise levels and noise types of frequency transfer using GPS CV, GPS CP and TWSTFT. The best transfer techniques are TWSTFT and GPS CP, which exhibit FTUs close to 1×10^{-16} at 30 days. However, improved frequency transfer is needed for future frequency standards that could have uncertainties in the low 10^{-17} range.

There is still much to be learned about the level and type of noise in frequency transfer. It is not clear what the balance is between WPN and FPN and to what extent different transfer techniques are correlated. Is there an annual cycle present and how large is it? To answer many of these questions a third independent transfer method is needed. Unfortunately, there is no immediate prospect for a practical and economical technique, with sufficient stability, to appear in the near future. TWSTFT over optical fibres offers considerable promise, but dedicated fibres covering long (intercontinental) distances are very expensive.

Acknowledgments

The authors thank P Tavella, A Godone and L Lorini from INRIM for the helpful discussions about the uncertainty on the frequency and V Zhang from NIST for the GPS and TWSTFT data. They also thank their colleagues at the USNO, PTB and METAS for use of the TWSTFT and GPS data and thank Christine Hackman for processing the GPS CP data.

References

- [1] Parker T E, Howe D A and Weiss M 1998 Accurate frequency comparisons at the 1×10^{-15} level *Proc. IEEE Int. Frequency Control Symp. (Pasadena, CA)* pp 265–72
- [2] Panfilo G and Parker T E 2007 A theoretical analysis of frequency uncertainty *Proc. Joint Meeting of the IEEE Int. Frequency Control Symp. and the 21st European Frequency and Time Forum (Geneva, Switzerland)* pp 805–10
- [3] Parker T E and Panfilo G 2007 Experimental analysis of frequency transfer uncertainty *Proc. Joint Meeting of the IEEE Int. Frequency Control Symp. and the 21st European Frequency and Time Forum (Geneva, Switzerland)* pp 891–6
- [4] Parker T E and Zhang V 2005 Sources of instabilities in two-way satellite time transfer *Proc. Joint Meeting of the IEEE Int. Frequency Control Symp. and Precise Time and Time Interval (Vancouver, Canada)* pp 745–51
- [5] 1993 *Guide to the Expression of Uncertainty in Measurement* (Geneva: International Organization for Standardization)
- [6] Cox D R and Miller H D 1972 *The Theory of Stochastic Processes* (London: Chapman and Hall)
- [7] Ross S 1996 *Stochastic Processes* (New York: Wiley)
- [8] Morris D, Douglas R J and Boulanger J-S 1994 The role of the hydrogen maser for the frequency transfer from cesium fountains *Japan. J. Appl. Phys.* **33** 1659–68
- [9] Ferre-Pikal E S, Camparo J R, Cutler L S, Maleki L, Riley W J, Stein S R, Thomas C, Walls F L and White J D 1997 Draft revision of IEEE STD 1139-1988 Standard definitions of physical quantities for fundamental frequency and time metrology—random instabilities *Proc. Int. Frequency Control Symp. (Orlando, FL)* pp 338–57
- [10] Allan D W 1987 Time and frequency (time-domain) characterization, estimation, and prediction of precision clocks and oscillators *IEEE Trans. Ultrason. Ferroelectr. Freq. Control* **34** 647–54
- [11] Brown R G and Hwang P Y C 1997 *Introduction to Random Signal and Applied Kalman Filtering* (New York: Wiley) chapter 1
- [12] Bendat J S and Piersol A G 1993 *Engineering Applications of Correlation and Spectral Analysis* 2nd edn (Canada: Wiley)
- [13] Greenhall C A 1991 Recipes for degrees of freedom of frequency stability estimator *IEEE Trans. Instrum. Meas.* **40** 994–9
- [14] Panfilo G 2006 The mathematical modelling of the atomic clock error with application to time scales and satellite systems *PhD Thesis* Politecnico di Torino, Italy
- [15] Galleani L, Sacerdote L, Tavella P and Zucca C 2003 A mathematical model for the atomic clock error *Metrologia* **40** S257–64
- [16] Chaffee J W 1987 Relating the Allan variance to the diffusion coefficients of a linear stochastic differential equation model for precision oscillators *IEEE Trans. Ultrason. Ferroelectr. Freq. Control* **34** 655–8
- [17] Zucca C and Tavella P 2005 The clock model and its relationship with the Allan and related variances *IEEE Trans. Ultrason. Ferroelectr. Freq. Control* **52** 289–96
- [18] Arnold L 1974 *Stochastic Differential Equations: Theory and Applications* (New York: Wiley)
- [19] Abramovitz M and Stegun I 1972 *Handbook of Mathematical Functions* (New York: Dover)
- [20] Godone A, Micalizio S and Levi F 2008 RF spectrum of a carrier with a random phase modulation of arbitrary slope *Metrologia* **45** 313–24
- [21] Hackman C, Levine J and Parker T E 2006 A long-term comparison of GPS carrier-phase frequency transfer and two-way satellite time/frequency transfer *Proc. 38th Annual Precise Time and Time Interval Meeting (Reston, VA)* pp 485–98
- [22] Lewandowski W, Matsakis D, Panfilo G and Tavella P 2006 The evaluation of uncertainties in [UTC – UTC(k)] *Metrologia* **43** 278–86
- [23] BIPM *Circular T*: monthly publication [online] <http://www.bipm.org/jsp/en/TimeFtp.jsp?TypePub=publication>

Supplementary Material (Web Version Only)

Appendix

1A Simulation results (Supplement to Section 2)

To verify the theoretical analysis in Section 2 we calculate $u_{\bar{y}(\tau)}$ from the standard deviation of frequency as a function of τ from simulated phase noise data and compare it to the results for $u_{\bar{y}(\tau)}$ obtained using the Allan deviation in (14), (18) and (22). We use two different methods to simulate the time deviation time series. The first is based on the use of stochastic processes and the second on the use of fractional differences. Details can be found in [1A - 3A].

The process starts with simulated phase data, from which the frequency data as a function of τ are obtained using (1). The standard deviation of the frequency at each τ is calculated to obtain the uncertainty.

Three different cases are considered:

1. white phase noise with a typical Allan deviation equal to $\sigma_y(\tau) = 7 \times 10^{-15}$ at 1 *day*.
2. white frequency noise with a typical Allan deviation equal to $\sigma_y(\tau) = 4 \times 10^{-16}$ at 1 *day*.
3. flicker phase noise with a typical Allan deviation equal to $\sigma_y(\tau) = 7.5 \times 10^{-15}$ at $\tau_0 = 1$

$$\text{day with } \omega_n = \frac{\pi}{\tau_0} = \frac{\pi}{86400 \text{ s}}.$$

The results for cases 1, 2 and 3 are shown in Figures 1A, 2A and 3A. For all three cases very good agreement is obtained between the frequency uncertainties obtained directly from the standard deviations, grey lines, and the uncertainties using the expressions based on the Allan deviations, dashed black lines.

2A Analysis using real data (Supplement to Section 2)

Real experimental data is generally not made up of pure, individual noise processes, as in the previous analysis on simulated data, so it is useful to analyze some real data. In this section we compare the results for the calculation of the FTU using the standard deviation on two real data sets to that obtained from the equations in Section 2.3 which are functions of the Allan deviation. One data set contains WFN and the other has a combination of WPN and FPN. Clean WFN is

not readily found in transfer processes over an extended period of time, so we will use data from a commercial cesium frequency standard measured with respect to UTC(NIST) for a good approximation of WFN. UTC(NIST) is generated from a maser ensemble so the noise is dominated by the caesium standard. For this analysis the frequency offset is removed. For white and flicker phase noise we use the TWSTFT – GPS common view double difference for NIST – PTB data. NIST is the National Institute of Standards and Technology in Boulder Colorado, USA, and PTB is the Physikalisch-Technische Bundesanstalt in Braunschweig Germany.

2.1A White frequency noise

Here we compare the true frequency uncertainty (standard deviation) with the result obtained from (18) by using cesium clock data with respect to the UTC(NIST) time scale (frequency offset removed). The white frequency data set for the caesium standard consists of 100 days of data with an interval of 12 minutes. As expected the Allan deviation of this data shows white frequency noise with $\sigma_y(\tau) = 2.46 \times 10^{-13}$ at $\tau_0 = 12$ minutes and a $\tau^{-1/2}$ time interval dependence. In Figure 4A we show, as grey stars, the true frequency uncertainty of this data obtained from the standard deviation, and compare it to the frequency uncertainty calculated from (18) shown as the black line. The frequency uncertainty obtained from the Allan deviation using (18) agrees very well with the true uncertainty.

2.2A White and flicker phase noise

White and flicker phase noise data were obtained from the TWSTFT minus GPS CV double difference for UTC(NIST) – UTC(PTB) over a 300 day interval with data taken about every two hours. This data is shown in Figure 5A. In Figure 6A we show the modified Allan deviation for the NIST – PTB data to illustrate the different noise components. In this case it is clear from the modified Allan deviation that the data are white phase noise out to about 1 day (slope is about $\tau^{-3/2}$) and flicker phase noise for larger τ as indicated by the slope of τ^{-1} . As shown in Section 4, a Time Deviation (TDEV) plot could also have been used to resolve the two noise types.

To evaluate the frequency uncertainties from (14) and (22) we have to determine the levels of the two noise types individually. This can be done from the data in Figure 6A using the intercepts of the two noise types at 7200 s. The white phase noise has an Allan deviation of

$\sigma_{y,WPN}(\tau) = 3.7 \times 10^{-13}$ for $\tau_0 = 7200$ s, and the flicker phase noise has an Allan deviation of about $\sigma_{y,FPN}(\tau) = 1.2 \times 10^{-13}$ for $\tau_0 = 7200$ s. In this case the uncertainty is given by the combination of these two noise types considered independently as shown in the following relation with the ω_n parameter equal to $\omega_n = \frac{\pi}{\tau_0} = \frac{\pi}{7200 \text{ s}}$.

$$u_{\bar{y}(\tau)}^2 = \left(0.79 \sigma_{y,FPN}^2(\tau) + \frac{2}{3} \sigma_{y,WPN}^2(\tau) \right) \quad (\text{A1})$$

Figure 7A shows as grey stars the true frequency uncertainty as a function of τ for the experimental data in Figure 5A as obtained from the standard deviation. The contribution of the white phase noise alone from (14) is shown as the dashed grey line and the flicker phase noise from (22) is shown as the dotted black line. Both of the noise types combined in (23) are shown as the black solid line. The agreement between the true FTU of the experimental data and that calculated from the combination of (14) and (22) is very good.

3A Confidence limits of $\sigma_{\hat{f}_t}(A, \tau)$ (Supplement to Section 3)

Here we will consider the confidence intervals for $\sigma_{\hat{f}_t}(A, \tau)$. To calculate the confidence intervals we will follow the same method which has been used for the calculation of the confidence interval for the Allan deviation [4A-6A]. In particular we know that for the Allan variance [4A] the ratio

$$U = \frac{\hat{\sigma}_{\hat{f}_t}^2(A, \tau)}{\sigma_{\hat{f}_t}^2(A, \tau)} \nu \quad (\text{A2})$$

has a chi square distribution with ν degrees of freedom, where $\hat{\sigma}_{\hat{f}_t}^2(A, \tau)$ is the estimator related to the statistic $\sigma_{\hat{f}_t}^2(A, \tau)$. Based on the properties of the chi square distribution and on $E(\hat{\sigma}_{\hat{f}_t}^2(A, \tau)) = \sigma_{\hat{f}_t}^2(A, \tau)$ we can estimate the degrees of freedom using the relation:

$$\nu = \frac{2(\sigma_{\hat{f}_t}^2(A, \tau))^2}{\text{Var}(\hat{\sigma}_{\hat{f}_t}^2(A, \tau))} \quad (\text{A3})$$

After calculating the degrees of freedom we can obtain the confidence intervals for (23) using:

$$\frac{V}{b} \hat{\sigma}_{ft}^2(A, \tau) < \sigma_{ft}^2(A, \tau) < \frac{V}{a} \hat{\sigma}_{ft}^2(A, \tau) \quad (\text{A4})$$

where a and b are the percentiles of the chi square distribution at the confidence level p considered (usually the confidence levels are 68 %, 95 % and 99 %). The problem is to calculate the mean and the variance of the first difference statistic (23) in the case of WPN, WFN and FPN. Following the method reported in [6A] we can use the following relation

$$Var(\hat{\sigma}_{ft}^2(A, \tau)) = \frac{2}{M} (\sigma_{ft}^2(A, \tau))^2 \left(1 + \frac{2}{M} \sum_{k=1}^{M-1} (M-k) \rho_k^2 \right), \quad (\text{A5})$$

where $k = j - i > 0$, $M = N - \tau$ and the correlation coefficient $\rho_{i,j}$ considering $Z_i = \frac{X_{i+\tau} - X_i}{\tau}$ is defined by

$$\rho_{i,j} = \frac{E(Z_i Z_j)}{E(Z_i^2)} \quad (\text{A6})$$

N is the number of the equally spaced samples of \bar{x}_i , which is the average phase over interval A .

Considering relation (A5), the degrees of freedom following (A2) are:

$$\nu = \frac{N - \tau}{1 + \frac{2}{N - \tau} \sum_{k=1}^{N-\tau-1} (N - \tau - k) \rho_k^2} \quad (\text{A7})$$

Following the method reported in [6A] it is possible to obtain the expression for the correlation coefficients $\rho_{i,j}$. Here we report only the final values for the degrees of freedom for WPN, WFN, and FPN:

$$1. \text{ WPN: } \nu = \frac{2(N - \tau)^2}{3N - 4\tau} \quad (\text{A8})$$

$$2. \text{ WFN: } \nu = \frac{6(N - \tau)^2 \tau}{2N - \tau + 4N\tau^2 - 5\tau^3} \quad (\text{A9})$$

$$3. \text{ FPN: } \nu = \frac{N - \tau}{1 + \frac{2}{N - \tau} \left(\sum_{k=1}^{\tau-1} (N - \tau - k) \rho_{k,1}^2 + \sum_{k=\tau+1}^{N-\tau-1} (N - \tau - k) \rho_{k,2}^2 + (N - 2\tau) \rho_{k,3}^2 \right)} \quad (\text{A10})$$

where the correlation coefficients are given by the following relations:

$$\begin{aligned}
\rho_{k,1} &= \frac{-2\log(k) + \log(\tau^2 - k^2) + 2Ci(\omega_n\tau) - Ci(\omega_n(k+\tau)) - Ci(\omega_n(\tau-k))}{2\gamma + 2\log(\omega_n\tau) - 2Ci(\omega_n\tau)} \quad \text{if } k < \tau \\
\rho_{k,2} &= \frac{-2\log(k) + \log(k^2 - \tau^2) + 2Ci(\omega_n\tau) - Ci(\omega_n(k+\tau)) - Ci(\omega_n(k-\tau))}{2\gamma + 2\log(\omega_n\tau) - 2Ci(\omega_n\tau)} \quad \text{if } k > \tau \\
\rho_{k,3} &= \frac{-\gamma - \log(\omega\tau) + \log(2) + 2Ci(\omega_n\tau) - Ci(2\omega_n\tau)}{2\gamma + 2\log(\omega_n\tau) - 2Ci(\omega_n\tau)} \quad \text{if } k = \tau
\end{aligned} \tag{A11}$$

and $Ci(x)$ is the Cosine integral function, γ is Euler's constant, and ω_n is the bandwidth. This parameter was discussed in Section 2.3.3 .

4A Using TDEV in an expression like (25), (Supplement to Section 5.2)

TDEV at τ_0 from two low noise clocks can be used to estimate the $u_A(k)_i$, and this can be used in an expression like (25) to estimate the frequency transfer uncertainty. For WPN, using $u_A(k)_i =$ TDEV at τ_0 , and $x = 1$ in (25) will give an exact value for the FTU. The situation is more complicated for FPN, as illustrated in Figure 8A. A time series of simulated flicker phase noise was generated with TDEV at $\tau_0 = 1$ day equal to 0.24 ns. This value was used for $u_A(k)_1$ and $u_A(k)_2$ in (25) with $x = 0.9$. The FTU using $\sigma_{fi}(A=1d, \tau)$ was calculated for the time series and is shown as (black) dots in Figure 8A. The solid (red) line overlapping the dots is a best straight line fit to this data with a log/log slope of -0.875. A careful inspection of the dotted curve shows that the slope is not constant. At small τ the slope is approximately -0.7 and increases to about -1 at large τ . The dashed line with (blue) hollow diamonds shows the result from (25). The overall slope from the equation is in good agreement with the fit to the curve with dots, but the FTU level from the equation is biased about 25 % low. The bias between the equation and the data point at $\tau_0 = 1$ day is only about 15 %, but the slope here is smaller than 0.9. Therefore, using a TDEV value for $u_A(k)$ in an expression such as that in (25) to estimate frequency transfer uncertainty for FPM noise is relatively complicated. The precise bias and exponent will depend on what range of τ (relative to τ_0) that one is interested in.

References

- [1A] L. Galleani, L. Sacerdote, P. Tavella, C. Zucca. “A mathematical model for the atomic clock error”, *Metrologia*, Vol. 40, pp. S257-S264, 2003.
- [2A] Lara S. Schmidt. Atomic clock models using fractionally integrated noise processes. *Metrologia*, vol. 40, S305-S311, 2003.
- [3A] Donald B. Percival. Stochastic models and statistical analysis for clock noise. *Metrologia*, vol. 40, S289-S304, 2003.
- [4A] M. A. Weiss, F.L. Walls, C.A. Greenhall, T. Walter. “Confidence on the modified Allan variance and the time variance”. in *Proc. of the European Frequency and Time Forum*, pp. 153-165, 1995 (Besancon, France).
- [5A] D.A. Howe, D. W. Allan and J. A. Barnes. “Properties of signal sources and Measurement methods”, in *Proc. of the 35th Annual Symposium on Frequency Control*, pp 1-47, 1981 (Philadelphia, PA, USA).
- [6A] C.A. Greenhall. “Recipes for degrees of freedom of frequency stability estimator”. *IEEE Transactions and Instrumentation and Measurement*, vol. 40, no.6, pp. 994-999, 1991.

Figure Captions

Figure 1A. The true fractional frequency uncertainty for simulated WPN as a function of τ obtained from the standard deviation is shown as the grey line and the uncertainty obtained from (14) using the Allan deviation is shown as the dashed black line.

Figure 2A. The true fractional frequency uncertainty for simulated WFN as a function of τ obtained from the standard deviation is shown with the gray line and the uncertainty obtained from (18) using the Allan deviation is shown with the the dashed black line.

Figure 3A. The true fractional frequency uncertainty for simulated FPN as a function of τ obtained from the standard deviation is shown with the grey line and the uncertainty obtained from (22) using the Allan deviation is shown with the dashed black line.

Figure 4A. The true fractional frequency uncertainty of WFN from a caesium clock obtained with the standard deviation shown as grey stars, compared to the results from (18) shown as the solid black line.

Figure 5A. Data showing the NIST – PTB link double difference of TWSTFT – GPS CV.

Figure 6A. The modified Allan deviation for the NIST – PTB link using TWSTFT minus GPS CV data.

Figure 7A. The frequency transfer uncertainty (standard deviation) obtained from the NIST – PTB data is shown by the grey stars. The uncertainty obtained from (22) for flicker phase noise is shown as the dotted black line, white phase noise from (14) is shown as the dashed grey line and both of these combined as the solid black line.

Figure 8A. Comparison of frequency transfer uncertainty for simulated flicker phase noise calculated from $\sigma_{ft}(A=1d,\tau)$, (black) dots, and equation (25), (blue) diamonds. Note that the log/log slope for the $\sigma_{ft}(A=1d,\tau)$ data is not constant as compared to the straight fit line (red).

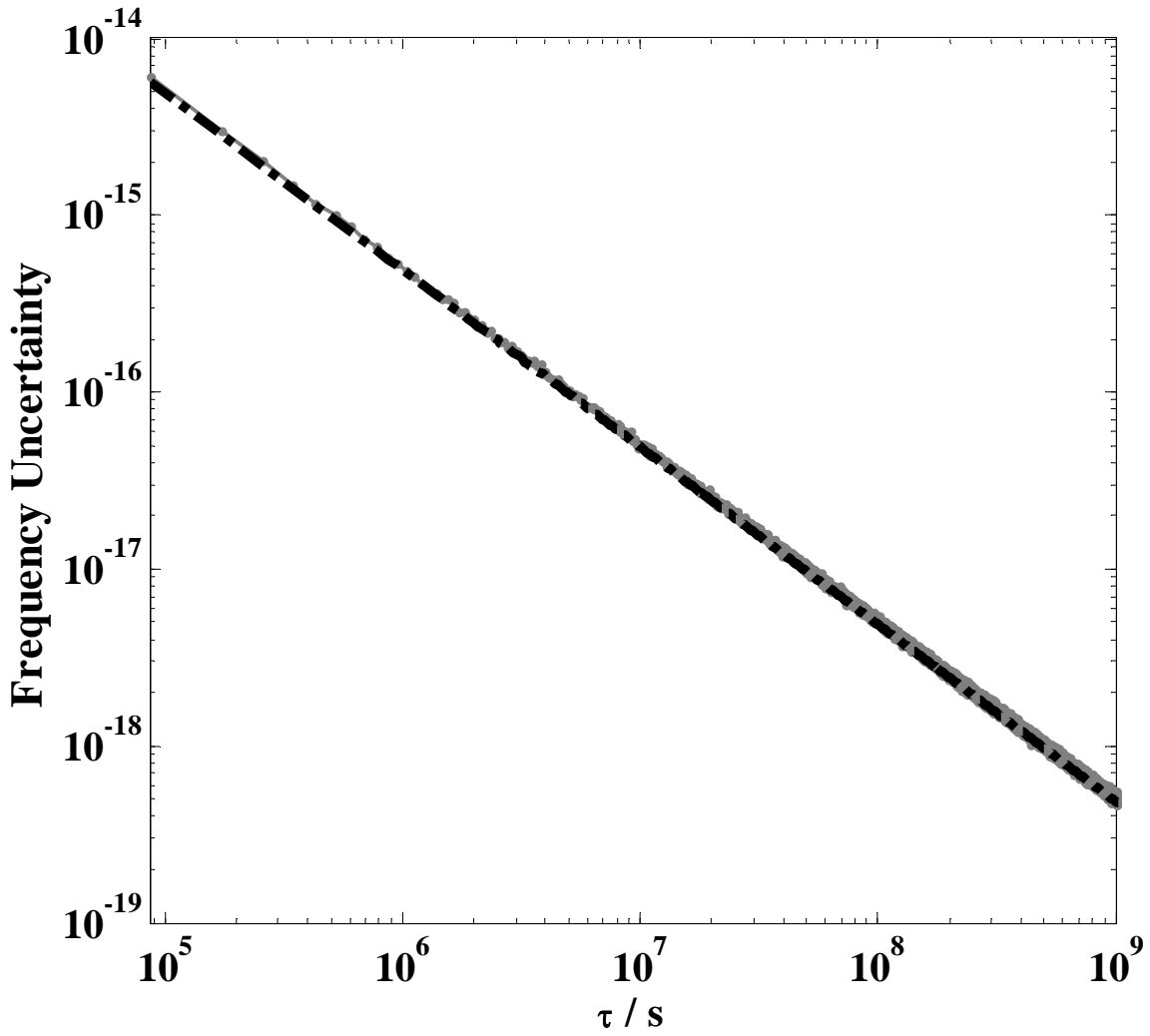


Figure 1A. The true fractional frequency uncertainty for simulated WPN as a function of τ obtained from the standard deviation is shown as the grey line and the uncertainty obtained from (14) using the Allan deviation is shown as the dashed black line.

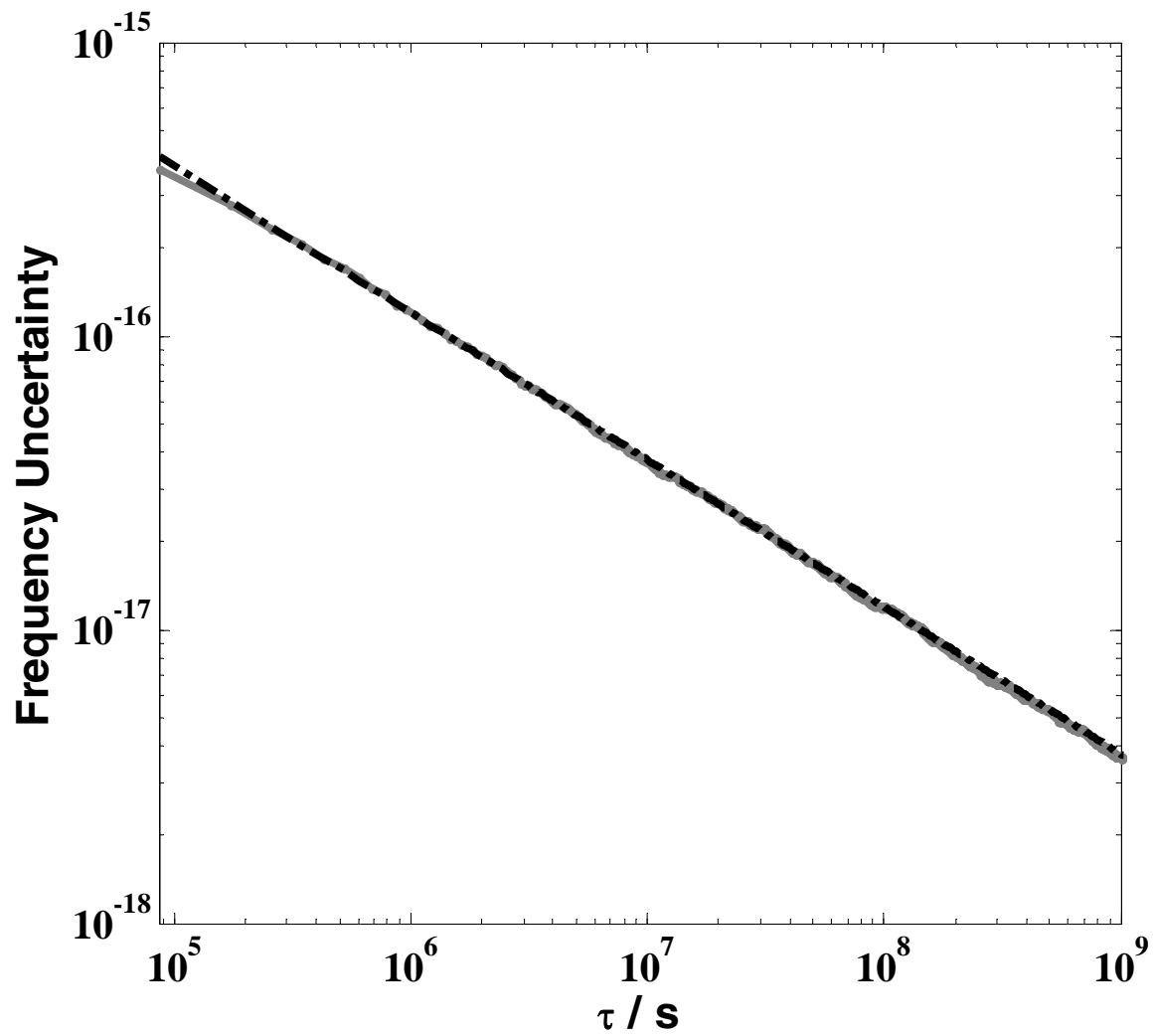


Figure 2A. The true fractional frequency uncertainty for simulated WFN as a function of τ obtained from the standard deviation is shown with the gray line and the uncertainty obtained from (18) using the Allan deviation is shown with the dashed black line.

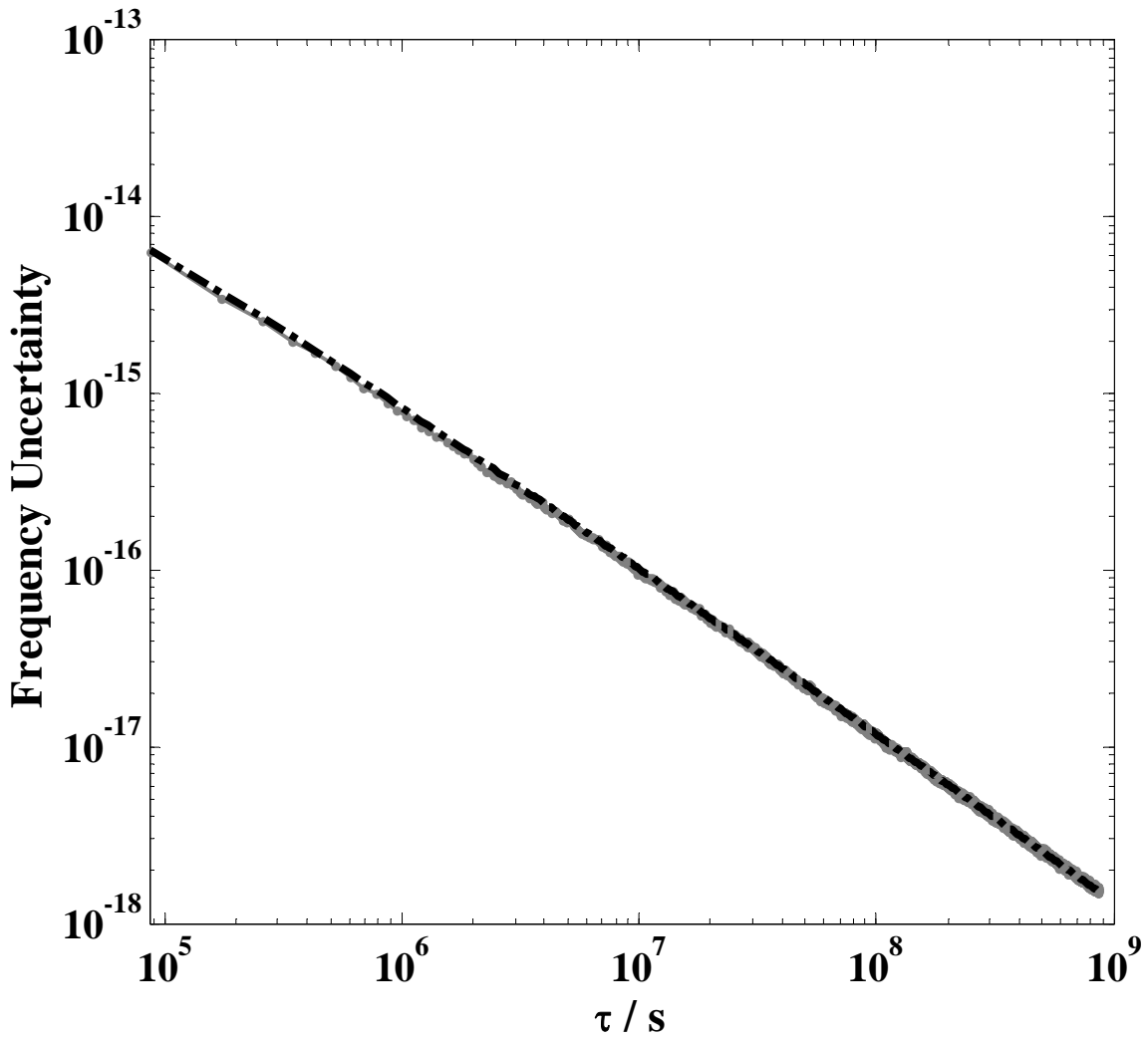


Figure 3A. The true fractional frequency uncertainty for simulated FPN as a function of τ obtained from the standard deviation is shown with the grey line and the uncertainty obtained from (22) using the Allan deviation is shown with the dashed black line.

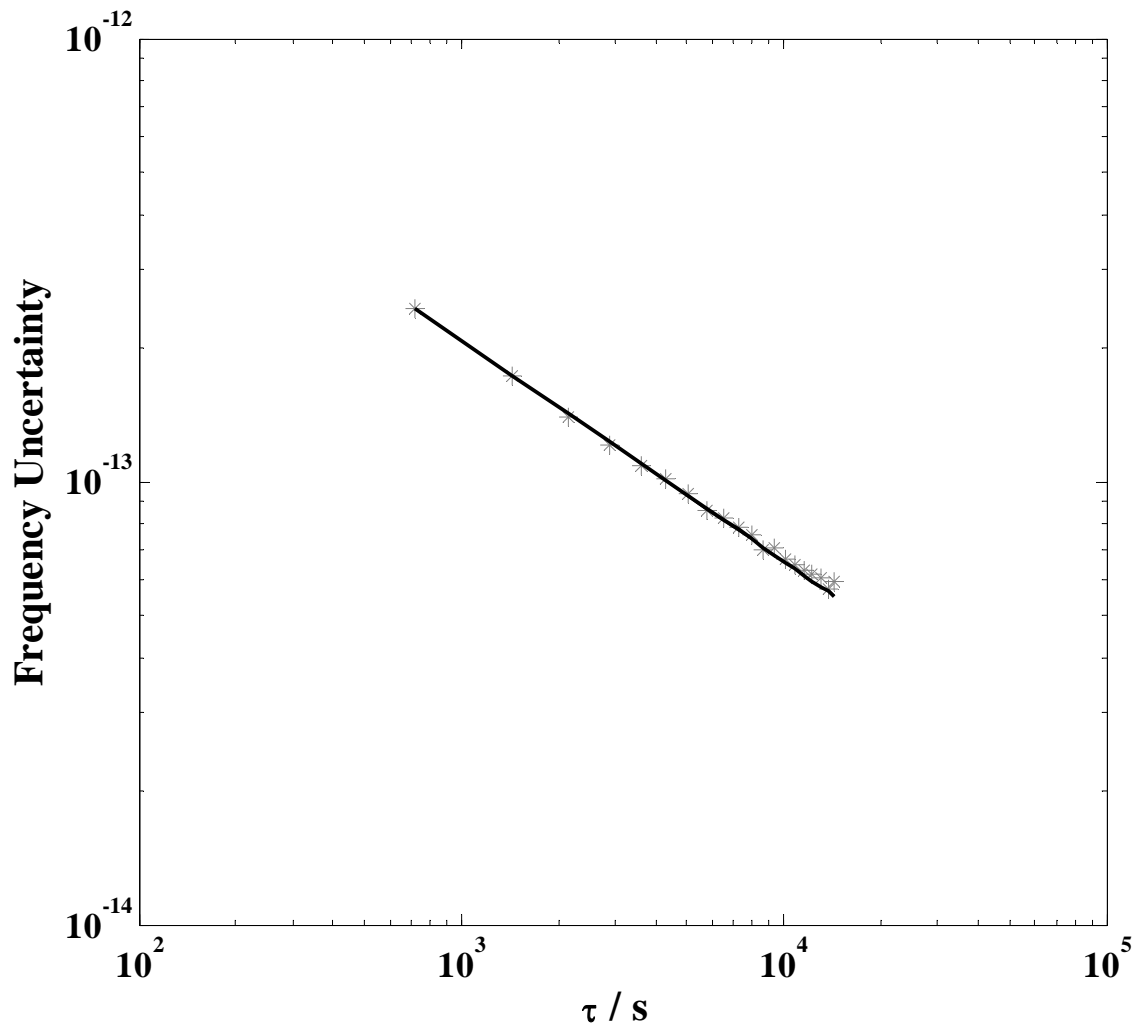


Figure 4A. The true fractional frequency uncertainty of WFN from a caesium clock obtained with the standard deviation, data shown as grey stars, compared to the results from (18) shown as the solid black line.

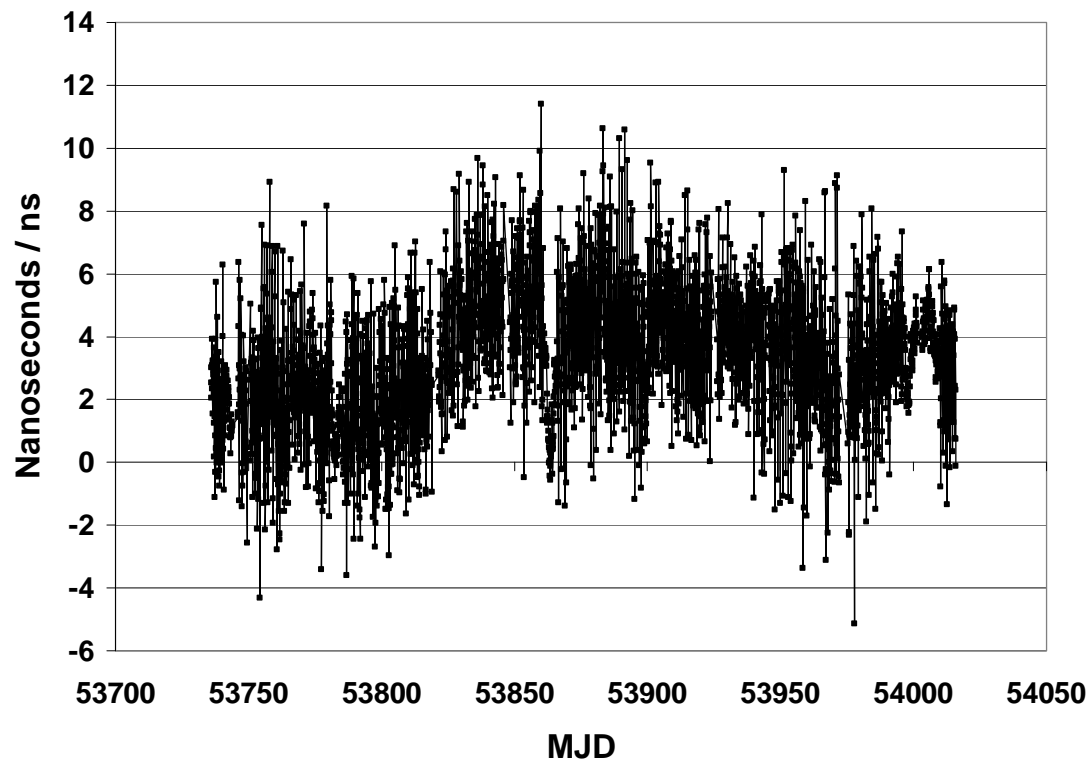
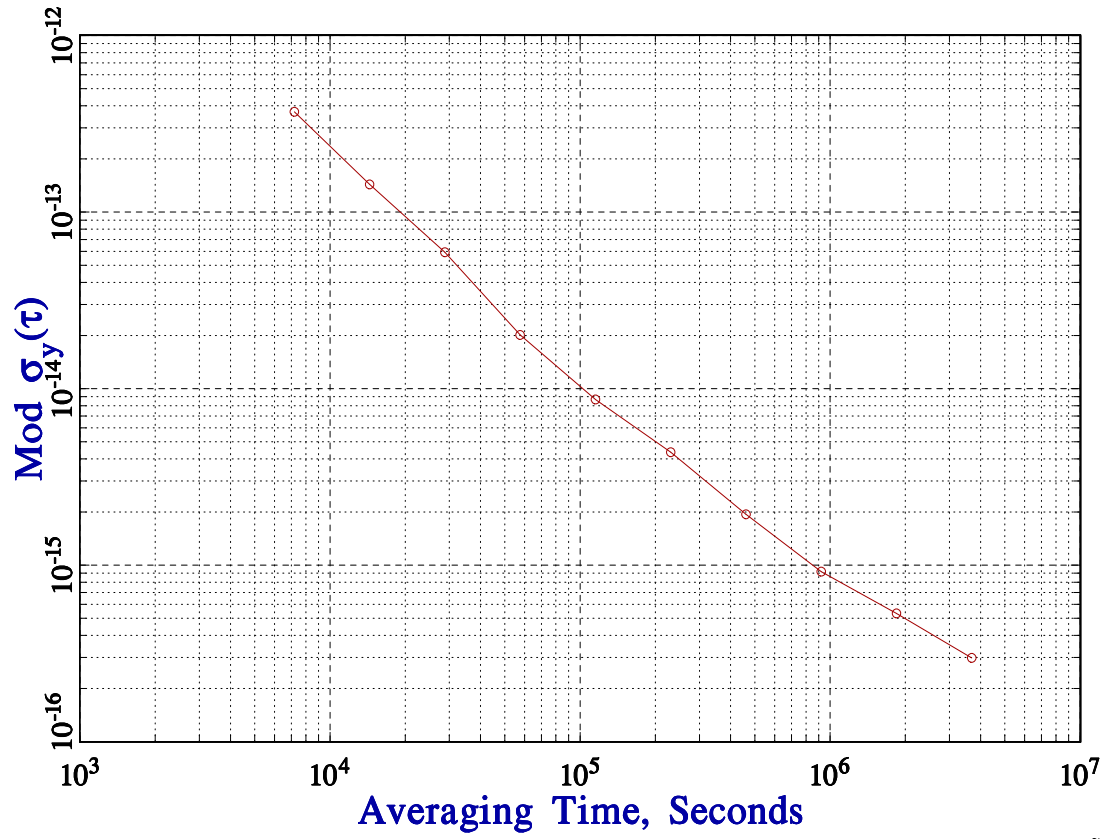


Figure 5A. Data showing the NIST-PTB link double difference of TWSTFT – GPS CV.

FREQUENCY STABILITY



Stable32

Figure 6A. The modified Allan deviation for the NIST-PTB link using TWSTFT minus GPS-CV data.

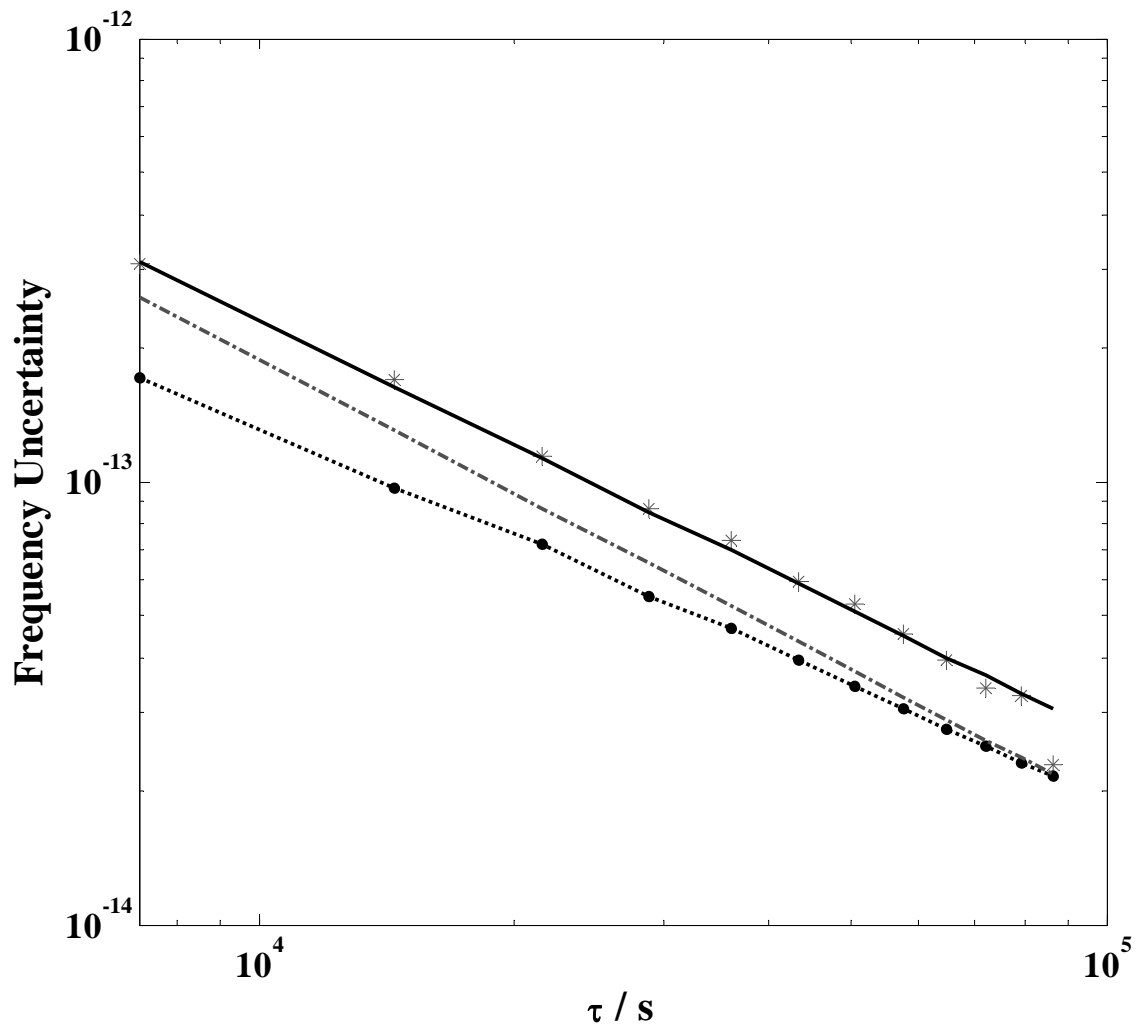


Figure 7A. The frequency transfer uncertainty (standard deviation) obtained from the NIST-PTB data is shown by the grey stars. The uncertainty obtained from (22) for flicker phase noise is shown as the dotted black line, white phase noise from (14) is shown as the dashed grey line and both of these combined as the solid black line.

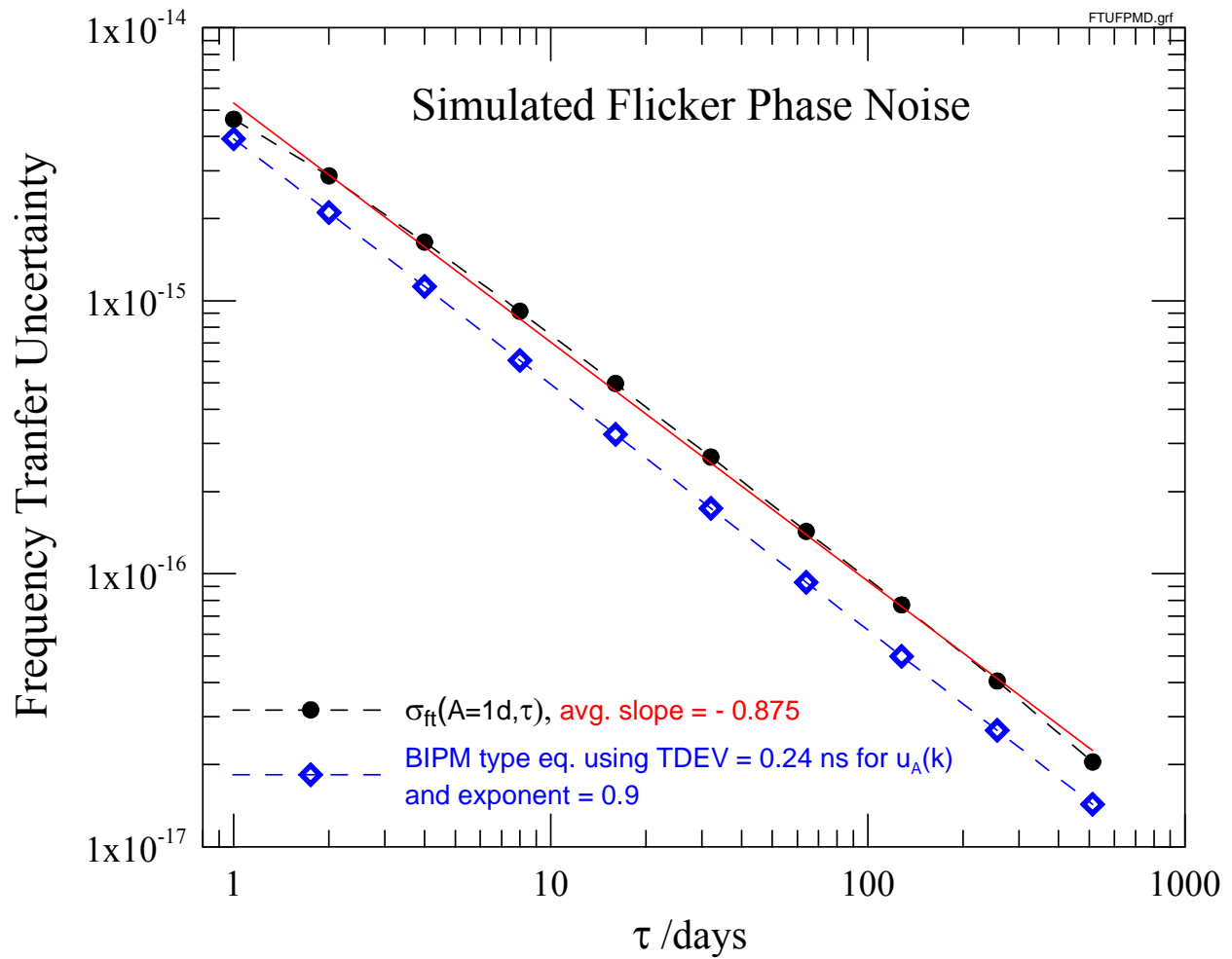


Figure 8A. Comparison of frequency transfer uncertainty for simulated flicker phase noise calculated from $\sigma_{ft}(A=1d, \tau)$, (black) dots, and equation (25), (blue) diamonds. Note that the log/log slope for the $\sigma_{ft}(A=1d, \tau)$ data is not constant as compared to the straight fit line (red).